

Feynman rules for the rational part of the Electroweak 1-loop amplitudes in the R_ξ gauge and in the Unitary gauge.

M.V. Garzelli

*Departamento de Física Teórica y del Cosmos y CAFPE Universidad de Granada,
E-18071 Granada, Spain and
INFN Milano, I-20133 Milano, Italy.
E-mail: garzelli@to.infn.it*

I. Malamos

*Department of Theoretical High Energy Physics, Institute for Mathematics, Astrophysics
and Particle Physics, Radboud Universiteit Nijmegen, 6525 AJ Nijmegen, the
Netherlands.
E-mail: J.Malamos@science.ru.nl*

R. Pittau

*Departamento de Física Teórica y del Cosmos y CAFPE Universidad de Granada,
E-18071 Granada, Spain.
E-mail: pittau@ugr.es*

ABSTRACT: We present the complete set of Feynman rules producing the rational terms of kind R_2 needed to perform any 1-loop calculation in the Electroweak Standard Model. Our formulae are given both in the R_ξ gauge and in the Unitary gauge, therefore completing the results in the 't Hooft-Feynman gauge already presented in a previous publication. As a consistency check, we verified, in the case of the process $H \rightarrow \gamma\gamma$ and in a few other physical cases, the independence of the total Rational Part ($R_1 + R_2$) on the chosen gauge. In addition, we explicitly checked the equivalence of the limits $\xi \rightarrow \infty$ after or before the loop momentum integration in the definition of the Unitary gauge at 1-loop.

KEYWORDS: NLO, radiative corrections, LHC, ILC, Electroweak interactions.

Contents

1. Introduction	1
2. Theory of R_2	2
3. Notations and Feynman rules	3
4. Results	5
4.1 The R_ξ gauge	6
4.1.1 Bosonic contribution to the vertices with 2 legs	6
4.1.2 Bosonic contribution to the vertices with 3 legs	9
4.1.3 Bosonic contribution to the vertices with 4 legs	9
4.2 The Unitary gauge	10
4.2.1 Bosonic contribution to the vertices with 2 legs	10
4.2.2 Bosonic contribution to the vertices with 3 legs	13
4.2.3 Bosonic contribution to the vertices with 4 legs	13
5. Checks	13
6. Conclusions	14

1. Introduction

The complete automation of the 1-loop calculations is nowadays a feasible task [1]. The advent of the OPP reduction method [2], together with the concept of multiple cuts [3], allowed to revitalize Unitarity [4] based Techniques, such as Generalized Unitarity (GU) [5], by reducing the computation of 1-loop amplitudes to a problem with the same conceptual complexity of a tree level calculation, resulting in achievements that were inconceivable only a few years ago [6]. As a matter of principle, any program capable of producing tree level results can be transformed nowadays into a NLO calculator by either *cutting* the 1-loop diagrams, in the OPP method, or by *gluing* tree level structures in the GU approach.

Both OPP and GU, when applied in 4 dimensions, allow the extraction of the Cut Constructible (CC) part of the amplitude, while a left over piece, the rational part R , needs to be derived separately. In the Generalized Unitarity approaches, this is achieved by computing the amplitude in different numbers of space-time dimensions, or via bootstrapping techniques [7], while, in the OPP approach, R is split in 2 pieces $R = R_1 + R_2$. The first piece, R_1 , is derivable in the same framework used to reconstruct the CC part of the amplitude, while R_2 is computable through a special set of Feynman rules for the theory at hand [8], to be used in a tree level-like computation.

The OPP treatment of R in its present formulation has one advantage and one drawback. The advantage is that no calculation in dimensions other than four is needed, avoiding the use of 6 and 8 dimensional explicit representations of the external particle wave functions. The drawback is that, for each theory that needs to be studied, a different special set of Feynman Rules has to be explicitly computed once for all. On the other hand, in the OPP framework, the speed for computing the Rational part is very high, so that we prefer it.

The full set of R_2 Feynman rules has been already derived for QED in [8], for QCD in [9], and, for the Standard Model (SM) of the Electroweak (EW) interactions in the 't Hooft-Feynman gauge in [10]. It is the main aim of the present paper to present the R_2 Feynman rules for the Electroweak Standard Model in a general renormalizable R_ξ gauge and in the Unitary gauge. On the one hand, this completes the theoretical picture on R_2 and, on the other hand, it allows tree level packages based on gauges other than the 't Hooft-Feynman one to be transformed into 1-loop calculators with the help of the mentioned OPP or GU techniques. In addition, the use of a general renormalizable R_ξ gauge, can be used to verify the correctness and the numerical stability of the 1-loop predictions by studying the invariance of the results under a change in the numerical value of ξ .

The outline of the paper is as follows. In section 2 we recall the origin of R_2 . In section 3 we fix our notation and our calculational framework. Section 4 contains the complete list of all possible special R_2 EW SM vertices in the R_ξ gauge and in the Unitary gauge. Finally, section 5 describes the tests we performed on our formulae.

2. Theory of R_2

The presence of a rational part R in a generic 1-loop amplitude is due to the regularization procedure needed before carrying out the calculation. In dimensional regularization, one computes the 1-loop integrals in $n = 4 + \epsilon$ dimensions, so that a generic m -point one-loop (sub-) amplitude reads

$$\mathcal{A} = \frac{1}{(2\pi)^4} \int d^n \bar{q} \frac{\bar{N}(\bar{q})}{\bar{D}_0 \bar{D}_1 \cdots \bar{D}_{m-1}}, \quad \bar{D}_i = (\bar{q} + p_i)^2 - m_i^2, \quad \bar{q} = q + \tilde{q}, \quad (2.1)$$

where \bar{q} is the integration momentum, a bar denotes objects living in n dimensions and a tilde represents ϵ -dimensional quantities. Notice that the external momenta p_i are always kept in 4 dimensions.

The numerator function $\bar{N}(\bar{q})$ can be split into a 4-dimensional plus an ϵ -dimensional part

$$\bar{N}(\bar{q}) = N(q) + \tilde{N}(\tilde{q}^2, q, \epsilon). \quad (2.2)$$

$N(q)$ brings information on the CC part of the amplitude (and within the OPP framework can also be used to compute a part of the rational piece called R_1), while $\tilde{N}(\tilde{q}^2, q, \epsilon)$ gives rise to a second piece of the rational part called R_2 , defined as

$$R_2 \equiv \frac{1}{(2\pi)^4} \int d^n \bar{q} \frac{\tilde{N}(\tilde{q}^2, q, \epsilon)}{\bar{D}_0 \bar{D}_1 \cdots \bar{D}_{m-1}}. \quad (2.3)$$

Due to possible ambiguities when passing from $N(q)$ to $\bar{N}(\bar{q})$, the actual form of $\tilde{N}(\tilde{q}^2, q, \epsilon)$ can only be read, to the best of our knowledge, starting from the original theory in n dimensions. In the OPP framework, that is achieved by computing analytically tree-level like Feynman rules, by splitting the Feynman diagrams according to the following three rules

$$\begin{aligned}\bar{q}_{\bar{\mu}} &= q_{\mu} + \tilde{q}_{\bar{\mu}} , \\ \bar{\gamma}_{\bar{\mu}} &= \gamma_{\mu} + \tilde{\gamma}_{\bar{\mu}} , \\ \bar{g}^{\bar{\mu}\bar{\nu}} &= g^{\mu\nu} + \tilde{g}^{\bar{\mu}\bar{\nu}} .\end{aligned}\tag{2.4}$$

Effective vertices are then generated by calculating the R_2 parts coming from all possible one-particle irreducible Green functions of the theory at hand, up to four external legs. The fact that four external legs are enough to account for R_2 is guaranteed by the ultraviolet nature of the rational terms, proved in [11]¹. Some freedom is however left in the choice of the regularization procedure, so that, instead of Eq. 2.3, one could also use the definition

$$R_2|_{FDH} = \frac{1}{(2\pi)^4} \int d^n \bar{q} \frac{\tilde{N}(\tilde{q}^2, q, \epsilon = 0)}{\bar{D}_0 \bar{D}_1 \cdots \bar{D}_{m-1}} ,\tag{2.5}$$

provided the same prescription is used in all parts of the calculation. The choice in Eq. 2.5 corresponds to the so called Four Dimensional Helicity scheme [12] (FDH). In such a scheme, when using dimensional regularization, the only object to be continued in n dimensions is

$$q^2 \rightarrow q^2 + \tilde{q}^2 ,\tag{2.6}$$

and it would be nice if one could be able to use this information to have access to R_2 starting uniquely from the theory in 4 dimensions. Unfortunately, the replacement in Eq. 2.6 is still too ambiguous, in the sense that different ways of writing $N(q)$ may lead to different n -dimensional continuations, as already observed in [10], so that no better solution can be found, at present, than relying on the original n -dimensional theory. It is worth mentioning that only the combination $R = R_1 + R_2$ is gauge invariant, not, in general, R_1 or R_2 separately. In this respect, the *right* analytical continuation from $N(q)$ to $\bar{N}(\bar{q})$ by means of Eq. 2.6, is that one that preserves all the Ward Identities of the theory.

In the following sections, we present the result of the explicit calculation we performed of all possible 2, 3 and 4-point effective vertices in the Electroweak Standard Model in a general R_{ξ} gauge and in the Unitary gauge.

3. Notations and Feynman rules

The vector boson fields (generically symbolized by V) are denoted by A , Z , W^{\pm} . The physical scalar Higgs field is written as H while χ and ϕ^{\pm} denote the neutral and the charged scalar goldstone bosons, respectively. All scalar fields are generically symbolized

¹In GU approaches, the entire calculation is instead performed in n dimensions, at the price of introducing, as already mentioned in the Introduction, explicit 6 and 8-dimensional polarization vectors for the particles glued together to form the loop amplitude.

by S . We work in the 1-fermion-family approximation, with lepton and quark doublets given by

$$\begin{pmatrix} \nu_l \\ l \end{pmatrix} \quad \text{and} \quad \begin{pmatrix} u \\ d \end{pmatrix}. \quad (3.1)$$

Fermions are generically symbolized by f , and the charge, the third isospin component and the mass of a fermion by Q_f , I_{3f} and m_f , respectively.

The sine and cosine of the Weinberg angle, the W and the Z mass are denoted by c_w , s_w , M_W and M_Z , respectively. Following reference [13], we introduce the two quantities V_{ud} and V_{du}^\dagger in the coupling of the W boson with the quark doublet of Eq. 3.1. This allows one to keep track of the CKM matrix and to easily generalize the results to the 3-families case. Finally, we use projector operators denoted by $\Omega^\pm = \frac{1 \pm \gamma_5}{2}$.

The set of Feynman rules we use for our calculation is that one given in [13], with some modifications due to the fact that the expressions in that paper refer to the 't Hooft-Feynman gauge, while we want to work in the R_ξ gauge. In the computation of R_2 , the ghost fields never enter, so that, in order to pass from the 't Hooft-Feynman gauge to the R_ξ one, we just need to modify the propagators of the scalar goldstone bosons and of the vector bosons as follows

$$S \overset{p}{\dashrightarrow} S = \frac{i}{p^2 - \xi M_S^2}$$

$$V_\alpha \overset{p}{\rightsquigarrow} V_\beta = \frac{-i}{p^2 - M_V^2} \left(g_{\alpha\beta} - (1 - \xi) \frac{p_\alpha p_\beta}{p^2 - \xi M_V^2} \right).$$

To compute our results in the Unitary gauge, we simply take the limit $\xi \rightarrow \infty$ in the above propagators *before integrating* over the loop momentum ². Then the unphysical scalar particles decouple and the massive gauge boson propagators become

$$\frac{-i}{p^2 - M_V^2} \left(g_{\alpha\beta} - \frac{p_\alpha p_\beta}{M_V^2} \right), \quad (3.2)$$

while for the photon we use

$$\frac{-i}{p^2} g_{\alpha\beta}. \quad (3.3)$$

Notice that the choice in Eq. 3.2 is mandatory in the framework of the OPP method. In fact, taking the limit $\xi \rightarrow \infty$ *after* integration over the loop momentum would imply a nonviable numerical cancellation between R_1 and R_2 , since the two parts are treated separately.

A last comment is in order with respect to our treatment of γ_5 in vertices containing fermionic lines. When computing all contributing Feynman diagrams, we pick up a

²See section 5 for more discussions on this issue.

$$\begin{aligned}
(a) \quad & S_1 \overset{\overrightarrow{p_1}}{\text{-----}} \bullet \text{-----} S_2 = \text{Vert}(S_1, S_2) \\
(b) \quad & V_\alpha \overset{\overrightarrow{p_1}}{\text{~~~~~}} \bullet \text{-----} S = \text{Vert}(V, S) \\
(c) \quad & V_{1\alpha} \overset{\overrightarrow{p_1}}{\text{~~~~~}} \bullet \text{~~~~~} V_{2\beta} = \text{Vert}(V_1, V_2) \\
(d) \quad & f_1 \overset{\overrightarrow{p_1}}{\text{-----}} \bullet \text{-----} \bar{f}_2 = \text{Vert}(f_1, f_2)
\end{aligned}$$

Figure 1: All possible 2-point vertices.

“special” vertex in the loop and anticommute all γ_5 ’s to reach it before performing the n -dimensional algebra, and, when a trace is present, we start reading it from this vertex. This treatment produces, in general, a term proportional to the totally antisymmetric ϵ tensor, whose coefficient may be different depending on the choice of the “special” vertex. However, when summing over all quantum numbers of each fermionic family, we checked that all contributions proportional to ϵ cancel.

4. Results

In this section, we present our results. We omit, in this paper, the gauge invariant contributions coming from fermion loops, because they can be recovered with the help of the formulae we already worked out in the case of the ’t Hooft-Feynman gauge in [10]. In fact, the fermion loop part can be easily separated from the rest since it always involves a sum \sum_i over fermions or fermion families. A parameter λ_{HV} is introduced in our formulae such that $\lambda_{HV} = 1$ corresponds to the ’t Hooft-Veltman scheme and $\lambda_{HV} = 0$ to the FDH scheme of eq. 2.5.

We explicitly write down, in this publication, all the formulae in the 2-point case, while, for the 3 the and 4-point vertices, we just classify the non vanishing ones. In fact the expression we obtained are rather lengthy, and there is no point in writing them down on paper. We rather provide the full set of results as FORM [14] files [15]. The notation used in those files closely follows that one introduced in the previous section. In Fig. 1-3 we present the generic non vanishing 2-point, 3-point and 4-point vertices that appear in our calculation, that also serve to further fix our notations.

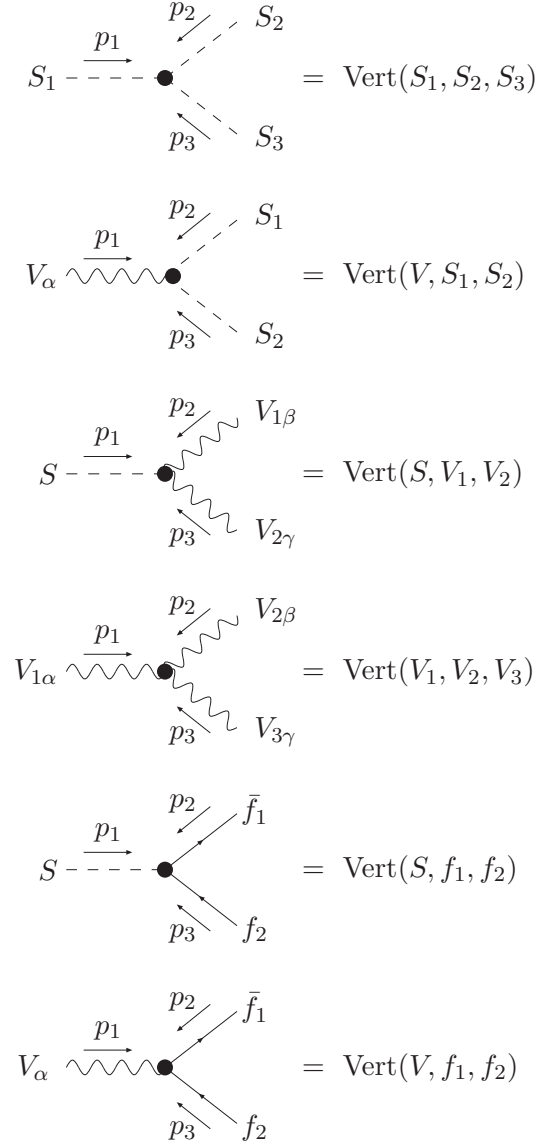


Figure 2: All possible non vanishing 3-point vertices.

4.1 The R_ξ gauge

4.1.1 Bosonic contribution to the vertices with 2 legs

Scalar-Scalar effective vertices

The generic effective vertex is

$$\text{Vert}(S_1, S_2) = \frac{ie^2}{16\pi^2 s_w^2} C \quad (4.1)$$

$$= \text{Vert}(S_1, S_2, S_3, S_4)$$

$$= \text{Vert}(S_1, S_2, V_1, V_2)$$

$$= \text{Vert}(V_1, V_2, V_3, V_4)$$

Figure 3: All possible non vanishing 4-point vertices.

with $\text{Vert}(S_1, S_2)$ given in fig. 1 (a) and with the actual values of S_1 , S_2 and C

$$\begin{aligned}
HH \quad : \quad C &= \frac{m_W^2}{4} (1 + 2\xi - \xi^2 - 12\lambda_{HV}) \left(1 + \frac{1}{2c_w^4}\right) + p_1^2 \frac{9 - 11\xi}{24} \left(1 + \frac{1}{2c_w^2}\right) \\
\chi\chi \quad : \quad C &= \frac{m_W^2}{24c_w^4} (1 + 2\xi^2 - 12\lambda_{HV}) + \frac{m_W^2}{12} (1 - 2\xi + 7\xi^2 - 12\lambda_{HV}) \\
&\quad - \frac{m_H^2}{12c_w^2} \left(1 - \frac{5}{2}\xi\right) + p_1^2 \frac{9 - 11\xi}{24} \left(1 + \frac{1}{2c_w^2}\right) \\
\phi^- \phi^+ \quad : \quad C &= \frac{m_W^2}{24c_w^4} (1 + 2\xi^2 - 12\lambda_{HV}) + \frac{m_W^2}{2c_w^2} \left(\xi - \frac{3}{2}\xi^2\right) \\
&\quad + \frac{m_W^2}{12} (1 - 8\xi + 16\xi^2 - 12\lambda_{HV}) \\
&\quad - \frac{m_H^2}{12} \left(1 - \frac{5}{2}\xi\right) + p_1^2 \frac{9 - 11\xi}{24} \left(1 + \frac{1}{2c_w^2}\right)
\end{aligned} \tag{4.2}$$

Vector-Scalar effective vertices

The generic effective vertex is

$$\text{Vert}(V, S) = \frac{ie^2}{\pi^2} C p_{1\alpha} \quad (4.3)$$

with $\text{Vert}(V, S)$ given in fig. 1 (b) and with the actual values of V , S and C

$$\begin{aligned} W^- \phi^+ & : C = -(1 - \xi) \frac{M_W}{192 c_w^2 s_w^2} \\ W^+ \phi^- & : C = (1 - \xi) \frac{M_W}{c_w^2 s_w^2} \\ Z \chi & : C = (1 - \xi) \frac{i M_Z}{192 c_w^2 s_w^2} (1 + 2 c_w^2 s_w^2) \\ A \chi & : C = (1 - \xi) \frac{i M_Z c_w}{96 s_w} \end{aligned} \quad (4.4)$$

Notice that all these vertices vanish in the 't Hooft-Feynman gauge ($\xi = 1$).

Vector-Vector effective vertices

The generic effective vertex is

$$\text{Vert}(V_1, V_2) = \frac{ie^2}{8\pi^2} (C_1 p_{1\alpha} p_{1\beta} + C_2 g_{\alpha\beta}) \quad (4.5)$$

with $\text{Vert}(V_1, V_2)$ given in fig. 1 (c) and with the actual values of V_1 , V_2 , C_1 and C_2

$$\begin{aligned} AA & : C_1 = K_1 \\ & C_2 = K_2 \\ AZ & : C_1 = -\frac{c_w}{s_w} K_1 \\ & C_2 = -\frac{c_w}{s_w} K_2 \\ ZZ & : C_1 = \frac{c_w^2}{s_w^2} K_1 \\ & C_2 = \frac{c_w^2}{s_w^2} K_2 \\ W^- W^+ & : C_1 = \frac{1}{s_w^2} K_1 \\ & C_2 = \frac{1}{s_w^2} K_2 \end{aligned} \quad (4.6)$$

where

$$\begin{aligned} K_1 &= -\frac{1}{3} \lambda_{HV} + \frac{3}{4} (1 - \xi) \\ K_2 &= p^2 \left(\frac{21\xi - 17}{24} + \frac{\lambda_{HV}}{3} \right) - \xi \frac{\xi + 3}{4} m_W^2 \end{aligned} \quad (4.7)$$

Fermion-Fermion effective vertices

The generic effective vertex is

$$\text{Vert}(f_1, f_2) = \frac{ie^2}{\pi^2} [(C_- \Omega^- + C_+ \Omega^+) \not{p}_1 + C_0] \quad (4.8)$$

with $\text{Vert}(f_1, f_2)$ given in fig. 1 (d) and with the actual values of f_1, f_2, C_-, C_+ and C_0

$$\begin{aligned} uu : \quad C_- &= \frac{Q_u^2}{c_w^2} \left(\frac{\lambda_{HV}}{16} - \frac{1-\xi}{24} \right) \\ C_+ &= \left(\frac{I_{3u}^2}{s_w^2 c_w^2} - \frac{2Q_u I_{3u}}{c_w^2} + \frac{Q_u^2}{c_w^2} + \frac{1}{2s_w^2} (V_{ud} V_{du}^\dagger) \right) \left(\frac{\lambda_{HV}}{16} - \frac{1-\xi}{24} \right) \\ C_0 &= \frac{m_u Q_u}{8c_w^2} (Q_u - I_{3u}) \left(\lambda_{HV} - \frac{1-\xi}{4} \right) \\ dd : \quad C_- &= \frac{Q_d^2}{c_w^2} \left(\frac{\lambda_{HV}}{16} - \frac{1-\xi}{24} \right) \\ C_+ &= \left(\frac{I_{3d}^2}{s_w^2 c_w^2} - \frac{2Q_d I_{3d}}{c_w^2} + \frac{Q_d^2}{c_w^2} + \frac{1}{2s_w^2} (V_{ud} V_{du}^\dagger) \right) \left(\frac{\lambda_{HV}}{16} - \frac{1-\xi}{24} \right) \\ C_0 &= \frac{m_d Q_d}{8c_w^2} (Q_d - I_{3d}) \left(\lambda_{HV} - \frac{1-\xi}{4} \right) \\ ll : \quad C_- &= \frac{Q_l^2}{c_w^2} \left(\frac{\lambda_{HV}}{16} - \frac{1-\xi}{24} \right) \\ C_+ &= \left(\frac{I_{3l}^2}{s_w^2 c_w^2} - \frac{2Q_l I_{3l}}{c_w^2} + \frac{Q_l^2}{c_w^2} + \frac{1}{2s_w^2} \right) \left(\frac{\lambda_{HV}}{16} - \frac{1-\xi}{24} \right) \\ C_0 &= \frac{m_l Q_l}{8c_w^2} (Q_l - I_{3l}) \left(\lambda_{HV} - \frac{1-\xi}{4} \right) \\ \nu_l \nu_l : \quad C_- &= 0 \\ C_+ &= \frac{1}{s_w^2} \left(\frac{I_{3\nu_l}^2}{c_w^2} + \frac{1}{2} \right) \left(\frac{\lambda_{HV}}{16} - \frac{1-\xi}{24} \right) \\ C_0 &= 0 \end{aligned} \quad (4.9)$$

4.1.2 Bosonic contribution to the vertices with 3 legs

The generic 3-point vertices appearing in our calculation are drawn in Fig. 2. As already pointed out, we limit ourselves to list the non vanishing cases, while the full set of results is available in [15]. We found 43 non zero R_2 vertices in the R_ξ gauge, classified in Table 1.

4.1.3 Bosonic contribution to the vertices with 4 legs

All non vanishing generic 4-point vertices that appear in our calculation are drawn in Fig. 3. The full set of results can be found in [15]. The 35 non zero R_2 vertices in the R_ξ gauge are classified in Table 2.

Scalar-Scalar-Scalar vertices:

$$\text{Vert}(H, H, H), \quad \text{Vert}(H, \chi, \chi), \quad \text{Vert}(H, \phi^+, \phi^-).$$

Vector-Scalar-Scalar vertices:

$$\begin{aligned} &\text{Vert}(A, H, \chi), \quad \text{Vert}(A, \phi^+, \phi^-), \quad \text{Vert}(Z, H, \chi), \quad \text{Vert}(Z, \phi^+, \phi^-), \\ &\text{Vert}(W^-, H, \phi^+), \quad \text{Vert}(W^-, \chi, \phi^+), \quad \text{Vert}(W^+, H, \phi^-), \quad \text{Vert}(W^+, \chi, \phi^-). \end{aligned}$$

Scalar-Vector-Vector vertices:

$$\begin{aligned} &\text{Vert}(H, A, A), \quad \text{Vert}(H, A, Z), \quad \text{Vert}(H, Z, Z), \quad \text{Vert}(H, W^+, W^-), \\ &\text{Vert}(\phi^-, A, W^+), \quad \text{Vert}(\phi^+, A, W^-), \quad \text{Vert}(\phi^-, Z, W^+), \quad \text{Vert}(\phi^+, Z, W^-). \end{aligned}$$

Vector-Vector-Vector vertices:

$$\text{Vert}(A, W^+, W^-), \quad \text{Vert}(Z, W^+, W^-).$$

Scalar-Fermion-Fermion vertices:

$$\begin{aligned} &\text{Vert}(H, u, u), \quad \text{Vert}(H, d, d), \quad \text{Vert}(H, l, l), \\ &\text{Vert}(\chi, u, u), \quad \text{Vert}(\chi, d, d), \quad \text{Vert}(\chi, l, l), \\ &\text{Vert}(\phi^-, d, u), \quad \text{Vert}(\phi^-, l, \nu_l), \quad \text{Vert}(\phi^+, u, d), \quad \text{Vert}(\phi^+, \nu_l, l). \end{aligned}$$

Vector-Fermion-Fermion vertices:

$$\begin{aligned} &\text{Vert}(A, u, u), \quad \text{Vert}(A, d, d), \quad \text{Vert}(A, \nu_l, \nu_l), \quad \text{Vert}(A, l, l), \\ &\text{Vert}(Z, u, u), \quad \text{Vert}(Z, d, d), \quad \text{Vert}(Z, \nu_l, \nu_l), \quad \text{Vert}(Z, l, l), \\ &\text{Vert}(W^-, d, u), \quad \text{Vert}(W^-, l, \nu_l), \quad \text{Vert}(W^+, u, d), \quad \text{Vert}(W^+, \nu_l, l). \end{aligned}$$

Table 1: The 43 non zero 3-point effective vertices in the R_ξ gauge. In the Unitary gauge there are 23 non vanishing vertices, namely the 22 listed here that do not contain χ or ϕ^\pm fields plus $\text{Vert}(H, \nu_l, \nu_l)$.

4.2 The Unitary gauge

We follow again the notations of Fig. 1.

4.2.1 Bosonic contribution to the vertices with 2 legs

Scalar-Scalar effective vertices

The generic effective vertex is

$$\text{Vert}(S_1, S_2) = \frac{ie^2}{16\pi^2 s_w^2} C \tag{4.10}$$

Scalar-Scalar-Scalar-Scalar vertices:

$$\begin{aligned} & \text{Vert}(H, H, H, H), \quad \text{Vert}(H, H, \chi, \chi), \quad \text{Vert}(H, H, \phi^-, \phi^+), \\ & \text{Vert}(\chi, \chi, \chi, \chi), \quad \text{Vert}(\chi, \chi, \phi^-, \phi^+), \quad \text{Vert}(\phi^-, \phi^+, \phi^-, \phi^+). \end{aligned}$$

Scalar-Scalar-Vector-Vector effective vertices:

$$\begin{aligned} & \text{Vert}(H, H, A, A), \quad \text{Vert}(H, H, A, Z), \quad \text{Vert}(H, H, Z, Z), \quad \text{Vert}(H, H, W^-, W^+), \\ & \text{Vert}(H, \phi^+, W^-, A), \quad \text{Vert}(H, \phi^+, W^-, Z), \quad \text{Vert}(\chi, \chi, A, A), \quad \text{Vert}(\chi, \chi, A, Z), \\ & \text{Vert}(\chi, \chi, Z, Z), \quad \text{Vert}(\chi, \chi, W^-, W^+), \quad \text{Vert}(\chi, \phi^+, W^-, A), \quad \text{Vert}(\chi, \phi^+, W^-, Z), \\ & \text{Vert}(\phi^-, H, A, W^+), \quad \text{Vert}(\phi^-, H, Z, W^+), \quad \text{Vert}(\phi^-, \chi, A, W^+), \quad \text{Vert}(\phi^-, \chi, Z, W^+), \\ & \text{Vert}(\phi^-, \phi^+, A, A), \quad \text{Vert}(\phi^-, \phi^+, A, Z), \quad \text{Vert}(\phi^-, \phi^+, Z, Z), \quad \text{Vert}(\phi^-, \phi^+, W^-, W^+). \end{aligned}$$

Vector-Vector-Vector-Vector effective vertices:

$$\begin{aligned} & \text{Vert}(A, A, A, A), \quad \text{Vert}(A, A, A, Z), \quad \text{Vert}(A, A, Z, Z), \\ & \text{Vert}(A, Z, Z, Z), \quad \text{Vert}(Z, Z, Z, Z), \quad \text{Vert}(A, A, W^-, W^+), \\ & \text{Vert}(A, Z, W^-, W^+), \quad \text{Vert}(Z, Z, W^-, W^+), \quad \text{Vert}(W^-, W^+, W^-, W^+). \end{aligned}$$

Table 2: The 35 non zero 4-point effective vertices in the R_ξ gauge. In the Unitary gauge there are 14 non vanishing vertices, namely all those ones that do not contain χ or ϕ^\pm fields.

with $\text{Vert}(S_1, S_2)$ given in fig. 1 (a) and with the actual values of S_1 , S_2 and C

$$HH \quad : \quad C = \frac{5}{6} p_1^2 \left(1 + \frac{1}{2c_w^2} \right) - \frac{9}{40} \frac{p_1^4}{m_W^2} - m_W^2 \left(1 + \frac{1}{2c_w^4} \right) \left(\frac{1}{4} + 3\lambda_{HV} \right) \quad (4.11)$$

Vector-Scalar effective vertices

No contribution is found in the Unitary gauge.

Vector-Vector effective vertices

The generic effective vertex is

$$\text{Vert}(V_1, V_2) = \frac{ie^2}{8\pi^2} (C_1 p_{1\alpha} p_{1\beta} + C_2 g_{\alpha\beta}) \quad (4.12)$$

with $\text{Vert}(V_1, V_2)$ given in fig. 1 (c) and with the actual values of V_1 , V_2 , C_1 and C_2

$$\begin{aligned} AA \quad : \quad & C_1 = K_1 \\ & C_2 = K_2 \end{aligned}$$

$$\begin{aligned} AZ \quad : \quad & C_1 = -\frac{c_w}{s_w} K_1 \\ & C_2 = -\frac{c_w}{s_w} K_2 \end{aligned}$$

$$\begin{aligned}
ZZ &: C_1 = \frac{c_w^2}{s_w^2} K_1 \\
&C_2 = \frac{c_w^2}{s_w^2} K_2 \\
W^- W^+ &: C_1 = \frac{1}{s_w^2} K_3 \\
&C_2 = \frac{1}{s_w^2} K_4
\end{aligned} \tag{4.13}$$

where

$$\begin{aligned}
K_1 &= -\frac{1}{3} (\lambda_{HV} - 5) - \frac{17}{60} \frac{p_1^2}{m_W^2} \\
K_2 &= \frac{3}{4} m_W^2 + \frac{1}{3} p_1^2 \left(\lambda_{HV} - \frac{23}{4} \right) + \frac{37}{120} \frac{p_1^4}{m_W^2} \\
K_3 &= -\frac{1}{3} \left(\lambda_{HV} - \frac{5}{2} - \frac{9}{8} c_w^2 \right) + \frac{11}{24} c_w^4 - \frac{17}{120} \frac{p_1^2}{m_W^2} (1 + c_w^4) \\
K_4 &= \frac{3}{8} \frac{m_W^2}{c_w^2} (s_w^2 + c_w^4 + c_w^6) + p_1^2 \left[\frac{\lambda_{HV}}{3} - \frac{7}{8} - \frac{7}{16} c_w^2 \left(1 + \frac{29}{21} c_w^2 \right) \right] \\
&\quad + \frac{37}{240} \frac{p_1^4}{m_W^2} (1 + c_w^4)
\end{aligned} \tag{4.14}$$

Fermion-Fermion effective vertices

The generic effective vertex is

$$\text{Vert}(f_1, f_2) = \frac{ie^2}{\pi^2} [(C_- \Omega^- + C_+ \Omega^+) \not{p}_1 + C_0] \tag{4.15}$$

with $\text{Vert}(f_1, f_2)$ given in fig. 1 (d) and with the actual values of f_1 , f_2 , C_- , C_+ and C_0

$$\begin{aligned}
uu &: C_- = \frac{Q_u^2}{16c_w^2} \left[\lambda_{HV} + \frac{s_w^2}{m_Z^2} \left(\frac{p_1^2}{4} - \frac{2}{3} m_Z^2 - \frac{5}{6} m_u^2 \right) \right] \\
C_+ &= \frac{\lambda_{HV}}{16} \left[\frac{I_{3u}^2}{s_w^2 c_w^2} - \frac{2Q_u I_{3u}}{c_w^2} + \frac{Q_u^2}{c_w^2} + \frac{1}{2s_w^2} (V_{ud} V_{du}^\dagger) \right] \\
&\quad + \frac{s_w^2}{16m_Z^2 c_w^2} \left(\frac{p_1^2}{4} - \frac{2}{3} m_Z^2 - \frac{5}{6} m_u^2 \right) \left(Q_u - \frac{I_{3u}}{s_w^2} \right)^2 \\
&\quad + \frac{V_{ud} V_{du}^\dagger}{32m_W^2 s_w^2} \left(\frac{p_1^2}{4} - \frac{2}{3} m_W^2 - \frac{5}{6} m_d^2 \right) \\
C_0 &= \frac{Q_u m_u}{8c_w^2} \left[\lambda_{HV} (Q_u - I_{3u}) + \frac{s_W^2}{4m_Z^2} \left(Q_u - \frac{I_{3u}}{s_w^2} \right) \left(\frac{p_1^2}{3} - m_Z^2 - m_u^2 \right) \right]
\end{aligned}$$

$$\begin{aligned}
dd : \quad C_- &= \frac{Q_d^2}{16c_w^2} \left[\lambda_{HV} + \frac{s_w^2}{m_Z^2} \left(\frac{p_1^2}{4} - \frac{2}{3}m_Z^2 - \frac{5}{6}m_d^2 \right) \right] \\
C_+ &= \frac{\lambda_{HV}}{16} \left[\frac{I_{3d}^2}{s_w^2 c_w^2} - \frac{2Q_d I_{3d}}{c_w^2} + \frac{Q_d^2}{c_w^2} + \frac{1}{2s_w^2} (V_{ud} V_{du}^\dagger) \right] \\
&\quad + \frac{s_w^2}{16m_Z^2 c_w^2} \left(\frac{p_1^2}{4} - \frac{2}{3}m_Z^2 - \frac{5}{6}m_d^2 \right) \left(Q_d - \frac{I_{3d}}{s_w^2} \right)^2 \\
&\quad + \frac{V_{ud} V_{du}^\dagger}{32m_W^2 s_w^2} \left(\frac{p_1^2}{4} - \frac{2}{3}m_W^2 - \frac{5}{6}m_u^2 \right) \\
C_0 &= \frac{Q_d m_d}{8c_w^2} \left[\lambda_{HV} (Q_d - I_{3d}) + \frac{s_W^2}{4m_Z^2} \left(Q_d - \frac{I_{3d}}{s_w^2} \right) \left(\frac{p_1^2}{3} - m_Z^2 - m_d^2 \right) \right] \\
ll : \quad C_- &= \frac{Q_l^2}{16c_w^2} \left[\lambda_{HV} + \frac{s_w^2}{m_Z^2} \left(\frac{p_1^2}{4} - \frac{2}{3}m_Z^2 - \frac{5}{6}m_l^2 \right) \right] \\
C_+ &= \frac{\lambda_{HV}}{16} \left[\frac{I_{3l}^2}{s_w^2 c_w^2} - \frac{2Q_l I_{3l}}{c_w^2} + \frac{Q_l^2}{c_w^2} + \frac{1}{2s_w^2} \right] \\
&\quad + \frac{s_w^2}{16m_Z^2 c_w^2} \left(\frac{p_1^2}{4} - \frac{2}{3}m_Z^2 - \frac{5}{6}m_l^2 \right) \left(Q_l - \frac{I_{3l}}{s_w^2} \right)^2 \\
&\quad + \frac{1}{32m_W^2 s_w^2} \left(\frac{p_1^2}{4} - \frac{2}{3}m_W^2 \right) \\
C_0 &= \frac{Q_l m_l}{8c_w^2} \left[\lambda_{HV} (Q_l - I_{3l}) + \frac{s_W^2}{4m_Z^2} \left(Q_l - \frac{I_{3l}}{s_w^2} \right) \left(\frac{p_1^2}{3} - m_Z^2 - m_l^2 \right) \right] \\
\nu_l \nu_l : \quad C_- &= 0 \\
C_+ &= \frac{\lambda_{HV}}{16s_w^2} \left(\frac{1}{2} + \frac{I_{3\nu_l}^2}{c_w^2} \right) + \frac{I_{3\nu_l}^2}{16m_Z^2 c_w^2 s_w^2} \left(\frac{p_1^2}{4} - \frac{2}{3}m_Z^2 \right) \\
&\quad + \frac{1}{32m_W^2 s_w^2} \left(\frac{p_1^2}{4} - \frac{2}{3}m_W^2 - \frac{5}{6}m_l^2 \right) \\
C_0 &= 0
\end{aligned} \tag{4.16}$$

4.2.2 Bosonic contribution to the vertices with 3 legs

The generic 3-point vertices appearing in our calculation are drawn in Fig. 2. As before the full set of results is available in [15]. We found 23 non zero R_2 vertices in the Unitary gauge, classified in Table 1.

4.2.3 Bosonic contribution to the vertices with 4 legs

All non vanishing generic 4-point vertices that appear in our calculation are drawn in Fig. 3. The full set of results is presented in [15]. The 14 non zero R_2 vertices in the Unitary gauge are classified in Table 2.

5. Checks

All our formulae have been obtained cross-checking two independent calculations. To

further check our results, we used the fact that the $R = R_1 + R_2$ contribution to physical quantities should be independent of the chosen gauge. In particular, parametrizing the gauge boson self-energies as follows

$$\Sigma_V^{\mu\nu}(p) = g^{\mu\nu} \Sigma_{V0}(p^2) + p^\mu p^\nu \Sigma_{V1}(p^2) \quad \text{with} \quad V = Z, W, \gamma, \quad (5.1)$$

we verified that the R contribution to $\Sigma_{W0}(M_W^2)$, $\Sigma_{Z0}(M_Z^2)$ and $\Sigma_{\gamma0}(0)$ is the same in both the R_ξ and the Unitary gauge. In addition, in the case of both gauges, we checked all of the 2-point like Ward Identities presented in [10] involving $\text{Vert}(S_1, S_2)$, $\text{Vert}(V, S)$ and $\text{Vert}(V_1, V_2)$.

To test the 3-point sector, we computed the $R = R_1 + R_2$ contribution to the process $H \rightarrow \gamma\gamma$. Again, we found the same answer working in both gauges, obtaining an expression for R in full agreement with that one presented in [16]. As for the 4-point sector, we checked that, in the limit $\xi \rightarrow 1$, we fully reproduce the effective vertices presented in [10].

Finally, in the case of the R_ξ gauge, we computed R_2 using both the following two equivalent representations for the massive gauge boson propagators

$$\begin{aligned} & -i \left(\frac{g_{\alpha\beta}}{p^2 - M_V^2} - (1 - \xi) \frac{p_\alpha p_\beta}{(p^2 - M_V^2)(p^2 - \xi M_V^2)} \right) \quad \text{and} \\ & -i \left(\frac{g_{\alpha\beta}}{p^2 - M_V^2} - \frac{p_\alpha p_\beta}{M_V^2(p^2 - M_V^2)} + \frac{p_\alpha p_\beta}{M_V^2(p^2 - \xi M_V^2)} \right), \end{aligned} \quad (5.2)$$

always finding the same results. Since the two expressions lead to different integrals in the intermediate stages of the calculation, this provides a strong consistency check of our procedure.

As a last remark notice that, when working in the Unitary gauge, we take the limit $\xi \rightarrow \infty$ *before* integrating over the loop momentum. The fact that this gives the same result for R as in a generic R_ξ gauge in the above mentioned cases *provided the same prescription is used in the calculation of R_1* is an explicit check of the equivalence of the limits $\xi \rightarrow \infty$ after or before the loop momentum integration in the definition of the Unitary gauge at 1-loop.

6. Conclusions

We presented the full set of Feynman rules producing the rational terms of kind R_2 needed to perform any 1-loop calculation in the Electroweak Standard Model in the R_ξ gauge and in the Unitary gauge. In a few physical cases we also checked the independence of the full rational piece $R = R_1 + R_2$ of the chosen gauge and, in the case of the Unitary gauge, of the order between the limit $\xi \rightarrow \infty$ and the integration over the loop momentum. Our results can be used to transform tree level packages based on gauges other than the 't Hooft-Feynman one into 1-loop calculators with the help of the OPP or Generalized Unitarity techniques.

Acknowledgments

R.P.'s and I.M.'s research was partially supported by the RTN European Programme MRTN-CT-2006-035505 (HEPTOOLS, Tools and Precision Calculations for Physics Discoveries at Colliders). M.V.G.'s research was supported by INFN. The research of R.P. and M.V.G. was also supported by the MEC project FPA2008-02984. R.P. also acknowledges the financial support of the bilateral INFN/MICINN program ACI2009-1045 (Aspects of Higgs physics at the LHC).

References

- [1] P. Mastrolia, G. Ossola, C. G. Papadopoulos and R. Pittau, JHEP **0806** (2008) 030 [arXiv:0803.3964 [hep-ph]];
T. Binoth, G. Ossola, C. G. Papadopoulos and R. Pittau, JHEP **0806** (2008) 082 [arXiv:0804.0350 [hep-ph]];
A. van Hameren, C. G. Papadopoulos and R. Pittau, JHEP **0909** (2009) 106 [arXiv:0903.4665 [hep-ph]];
R. K. Ellis, K. Melnikov and G. Zanderighi, JHEP **0904** (2009) 077 [arXiv:0901.4101 [hep-ph]];
C. F. Berger *et al.*, Phys. Rev. Lett. **102** (2009) 222001 [arXiv:0902.2760 [hep-ph]];
T. Binoth *et al.*, Comput. Phys. Commun. **181** (2010) 1612 [arXiv:1001.1307 [hep-ph]];
J. R. Andersen *et al.* [SM and NLO Multileg Working Group], arXiv:1003.1241 [hep-ph];
P. Mastrolia, G. Ossola, T. Reiter and F. Tramontano, JHEP **1008** (2010) 080 [arXiv:1006.0710 [hep-ph]];
R. Pittau, arXiv:1006.3773 [hep-ph];
G. Heinrich, G. Ossola, T. Reiter and F. Tramontano, arXiv:1008.2441 [hep-ph].
- [2] F. del Aguila and R. Pittau, JHEP **0407** (2004) 017 [arXiv:hep-ph/0404120];
R. Pittau, arXiv:hep-ph/0406105;
G. Ossola, C. G. Papadopoulos and R. Pittau, Nucl. Phys. B **763** (2007) 147 [arXiv:hep-ph/0609007];
G. Ossola, C. G. Papadopoulos and R. Pittau, JHEP **0803** (2008) 042 [arXiv:0711.3596 [hep-ph]].
- [3] R. Britto, F. Cachazo and B. Feng, Nucl. Phys. B **725** (2005) 275 [arXiv:hep-th/0412103].
- [4] Z. Bern, L. J. Dixon and D. A. Kosower, Phys. Rev. Lett. **70** (1993) 2677 [arXiv:hep-ph/9302280];
Z. Bern, L. J. Dixon, D. C. Dunbar and D. A. Kosower, Nucl. Phys. B **425** (1994) 217 [arXiv:hep-ph/9403226];
Z. Bern, L. J. Dixon, D. C. Dunbar and D. A. Kosower, Nucl. Phys. B **435**, 59 (1995) [arXiv:hep-ph/9409265];
Z. Bern, L. J. Dixon and D. A. Kosower, Nucl. Phys. B **437** (1995) 259 [arXiv:hep-ph/9409393];
- [5] Z. Bern and A. G. Morgan, Nucl. Phys. B **467**, 479 (1996) [arXiv:hep-ph/9511336];
Z. Bern, L. J. Dixon and D. A. Kosower, Nucl. Phys. B **513** (1998) 3 [arXiv:hep-ph/9708239];
C. Anastasiou, R. Britto, B. Feng, Z. Kunszt and P. Mastrolia, Phys. Lett. B **645** (2007) 213 [arXiv:hep-ph/0609191];
D. Forde, Phys. Rev. D **75**, 125019 (2007) [arXiv:0704.1835 [hep-ph]];

- W. T. Giele, Z. Kunszt and K. Melnikov, JHEP **0804** (2008) 049 [arXiv:0801.2237 [hep-ph]];
R. K. Ellis, W. T. Giele, Z. Kunszt and K. Melnikov, Nucl. Phys. B **822** (2009) 270
[arXiv:0806.3467 [hep-ph]].
- [6] G. Ossola, C. G. Papadopoulos and R. Pittau, JHEP **0707** (2007) 085 [arXiv:0704.1271
[hep-ph]];
G. Bevilacqua, M. Czakon, C. G. Papadopoulos, R. Pittau and M. Worek, JHEP **0909**
(2009) 109 [arXiv:0907.4723 [hep-ph]];
G. Bevilacqua, M. Czakon, C. G. Papadopoulos and M. Worek, Phys. Rev. Lett. **104** (2010)
162002 [arXiv:1002.4009 [hep-ph]];
T. Melia, K. Melnikov, R. Rontsch and G. Zanderighi, arXiv:1007.5313 [hep-ph];
C. F. Berger *et al.*, arXiv:1009.2338 [hep-ph].
- [7] Z. Bern, L. J. Dixon and D. A. Kosower, Phys. Rev. D **71**, 105013 (2005)
[arXiv:hep-th/0501240];
Z. Bern, L. J. Dixon and D. A. Kosower, Phys. Rev. D **72**, 125003 (2005)
[arXiv:hep-ph/0505055];
Z. Bern, L. J. Dixon and D. A. Kosower, Phys. Rev. D **73**, 065013 (2006)
[arXiv:hep-ph/0507005];
C. F. Berger, Z. Bern, L. J. Dixon, D. Forde and D. A. Kosower, Phys. Rev. D **74**, 036009
(2006) [arXiv:hep-ph/0604195].
- [8] G. Ossola, C. G. Papadopoulos and R. Pittau, JHEP **0805** (2008) 004 [arXiv:0802.1876
[hep-ph]].
- [9] P. Draggiotis, M. V. Garzelli, C. G. Papadopoulos and R. Pittau, JHEP **0904** (2009) 072
[arXiv:0903.0356 [hep-ph]].
- [10] M. V. Garzelli, I. Malamos and R. Pittau, JHEP **1001** (2010) 040 [arXiv:0910.3130 [hep-ph]].
- [11] T. Binoth, J. P. Guillet and G. Heinrich, JHEP **0702** (2007) 013 [arXiv:hep-ph/0609054];
A. Bredenstein, A. Denner, S. Dittmaier and S. Pozzorini, JHEP **0808** (2008) 108
[arXiv:0807.1248 [hep-ph]].
- [12] Z. Kunszt, A. Signer and Z. Trocsanyi, Nucl. Phys. B **411** (1994) 397 [arXiv:hep-ph/9305239];
S. Catani, M. H. Seymour and Z. Trocsanyi, Phys. Rev. D **55** (1997) 6819
[arXiv:hep-ph/9610553];
Z. Bern, A. De Freitas, L. J. Dixon and H. L. Wong, Phys. Rev. D **66** (2002) 085002
[arXiv:hep-ph/0202271].
- [13] A. Denner, Fortsch. Phys. **41** (1993) 307 [arXiv:0709.1075 [hep-ph]].
- [14] J. A. M. Vermaseren, arXiv:math-ph/0010025;
J. A. M. Vermaseren, Nucl. Phys. Proc. Suppl. **183** (2008) 19 [arXiv:0806.4080 [hep-ph]].
- [15] The FORM files with our results can be downloaded from
<http://www.ugr.es/local/pittau/CutTools>.
- [16] D. Y. Bardin and G. Passarino, *Oxford, UK: Clarendon (1999) 685 p.*